Canadian Mineralogist
Vol. 22, pp. 659-667 (1984)

Al–Si ORDERING IN 1M TRIOCTAHEDRAL MICAS

RICHARD N. ABBOTT, JR.

Department of Geology, Appalachian State University, Boone, North Carolina 28608, U.S.A.

ABSTRACT

The electron-diffraction pattern for a sample of biotite (1*M*-trioctahedral) shows weak diffractions violating the *C*-centring of the most commonly reported space-group $C2/m$. Al-Si ordering in trioctahedral micas, for which Al:Si is 1:3, is likely on a unit-cell scale only in the space groups $P2$, $P\bar{1}$, $P\bar{1}'$ and $P2_1$. There are two distinct Al-Si ordered primitive centrosymmetric triclinic structures, here designated $P\bar{1}$ and $P\bar{1}'$. Taking into account the principle of aluminum avoidance and other crystal-chemical considerations, the order of these space groups, from most favorable to least, is $P2_1$, $P\bar{1}$, $P2 \simeq P\bar{1}'$. There are four complexions of the $P2_1$ structure. Domains of the different $P2_1$ complexions would be related by reflection twinning, rotation twinning or inversion twinning. If the domains are very small, X-ray-diffraction and even electron-diffraction patterns may suggest the pseudosymmetry $C2/m$.

Keywords: biotite, trioctahedral micas, Al–Si ordering.

SOMMAIRE

Le cliché de diffraction électronique d'un échantillon de biotite 1*M* montre des taches de faible intensité en violation de la condition de la face C centrée du groupe spatial $C2/m$, le plus fréquemment attribué aux micas trioctaédriques. On s'attend à une mise en ordre des atomes Al et Si à l'échelle de la maille élémentaire dans de tels micas, dont le rapport Al:Si est de 1:3, seulement dans les groupes spatiaux $P2$, $P\bar{1}$, $P\bar{1}'$ et $P2_1$. On distingue deux structures tricliniques primitives centrosymétriques à Al et Si ordonnés: $P\bar{1}$ et $P\bar{1}'$. Une considération du principe de l'évitement des tétraèdres AlO_4 contigus et autres considérations d'ordre cristallochimique permettent de placer les quatre groupes spatiaux dans l'ordre suivant de stabilité: $P2_1$ (favorisé), $P\bar{1}$, $P2 \simeq P\bar{1}'$. Il y a quatre complexions de la structure $P2_1$. Les domaines de complexion différente dans cette structure seraient maclés par réflection, par rotation ou par inversion. Si les domaines sont de très petite taille, les clichés de diffraction X et de diffraction électronique pourraient simuler la pseudosymétrie $C2/m$.

(Traduit par la Rédaction)

Mots-clés: biotite, micas trioctaédriques, degré d'ordre Al-Si.

INTRODUCTION

The space group for most 1*M* trioctahedral micas has been reported as $C2/m$ (Deer *et al.* 1963); it is the basis for several structural refinements (Hazen & Burnham 1973, McCauley *et al.* 1973, Takeda & Morosin 1975, Takeda & Ross 1975). Biotite from a pegmatite, whose locality is unknown, was examined in this study by transmission-electron microscopy (TEM). The composition of the biotite is reported in Table 1. The *c*-axis diffraction pattern (Fig. 1) shows several violations of the *C*-centring in space group $C2/m$. The violations are weak, diffuse diffractions of the type *hk*0 where $h + k$ is odd, including (320), (140), (340), (540), (270), (470), (670), (870), (1,10,0), (3,10,0) (5,10,0) and the *mm*2 symmetrically related diffractions. The strongest of these are the types (270), (340), (140) and (1,10,0), in decreasing order of intensity. Except for the (270), even these are difficult to see in Figure 1, but are clearly visible on the negatives. The diffraction pattern shown in Figure 1 is not precisely centred, but by examining several near *c*-axis patterns, it appears that the Laue symmetry is *mm*2, consistent with the space groups $P2/m$, $P2_1/m$, $P2/a$, $P2_1/a$, $P2$, Pm, Pa or $P2_1$. It is the purpose of this paper to con-

TABLE 1. COMPOSITION OF BIOTITE[1] (AVERAGE OF 7 ANALYSES)

Wt. % oxide			Atoms per 11 oxygens		
SiO_2	35.96	(1.30)[2]	Si	2.762	4.00
TiO_2	3.03	(0.11)	Al	1.238	
Al_2O_3	19.28	(0.54)			
Cr_2O_3	0.04	(0.02)	Ti	0.173	2.694
[3]FeO	20.70	(0.58)	Al	0.507	
MnO	0.22	(0.04)	Cr	0.002	
MgO	5.85	(0.15)	Fe	1.330	
CaO	0.05	(0.01)	Mn	0.013	
K_2O	8.95	(0.25)	Mg	0.662	
Na_2O	0.49	(0.08)			
TOTAL	94.58		Ca	0.002	0.951
			K	0.877	
			Na	0.072	
			TOTAL	7.645	

[1] The analyses were performed by H.Y. McSween, Jr. on an MAC 400-S electron microprobe at the University of Tennessee, Knoxville.

[2] Standard deviation (1 sigma).

[3] All Fe reported as FeO.

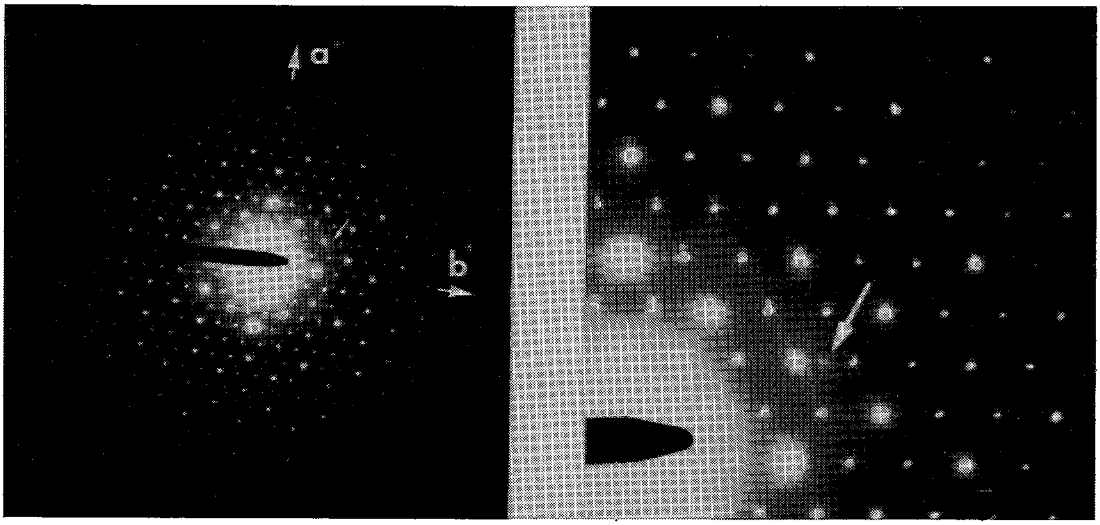

FIG. 1. Electron-diffraction pattern of biotite. Note the weak diffuse diffractions (marked by arrows) violating the C-centring. The arrow marks the (270) diffraction. Electron acceleration 100 kV.

sider the possible consequences of reduced symmetry, especially with regard to Al–Si order in the biotite just discussed and in trioctahedral micas in general.

The problem is addressed by introducing an Ordering Factor, OF, for the purpose of discriminating between different schemes of Al–Si ordering. The OF is simply calculated from the cell parameters and is purely geometrical. The bases for discriminating between different ordering schemes are the aluminum-avoidance principle (Loewenstein 1954) and charge-balance considerations discussed by Güven (1971).

Loewenstein's (1954) aluminum-avoidance principle asserts that two tetrahedral sites sharing an oxygen atom in a structure are not likely to be both occupied by aluminum. Furthermore, the distance between tetrahedral sites occupied by aluminum tends to be maximized. The principle follows from Pauling's (1960) rules and is satisfied in many structures, including feldspars, nepheline, kalsilite, margarite and sillimanite. For micas, Güven (1971) argued further that two apical oxygen atoms of Al-tetrahedra along the same shared octahedral edge would be especially unfavorable with respect to local balancing of electrostatic charge.

Gatineau (1964) and Gatineau & Méring (1966) have reported *non*-Bragg diffractions and streaked diffractions for muscovite, phlogopite and biotite. They suggested short-range ordering of tetrahedrally co-ordinated cations as a possible cause.

UNIT-CELL GEOMETRY

Figure 2a is an idealized (001) projection of the tetrahedral sites in one unit cell of a $1M$ mica (Pabst 1955). The octahedral cation sites between the sheets of tetrahedra and the large cation sites (K, Na, Ca) have been omitted in order to emphasize the geometrical relationship between the sheets of tetrahedra. The maximum symmetry is $C2/m$, in which all tetrahedral sites (labeled 1, 2, 3, 4 in the upper sheet and 1′, 2′, 3′, 4′ in the lower sheet) are symmetrically equivalent. For the $C2/m$ trioctahedral micas such as biotite or phlogopite, in which Al:Si is 1:3, the Al and Si must be disordered over the 8 equivalent tetrahedral sites, such that the probability of finding an Al atom on any one site is 25%. Figures 2b, c and d illustrate other C-centred structures compatible with the diffraction symmetry $C2/m$. In Cm, there are two types of tetrahedral sites, but all sites in one sheet are equivalent, $T1 = T2 = T3 = T4$ and $T1' = T2' = T3' = T4'$. Al–Si ordering in this structure would necessarily place more aluminum in one sheet than in the other, a possibility for which there is very little justification. The $C2$ structure has two sites, $T1 = T1' = T3 = T3'$ and $T2 = T2' = T4 = T4'$. The structure is compatible with the aluminum-avoidance principle. In the $2M_1$ dioctahedral mica *margarite*, the Al and Si (Al:Si = 1) are ordered in this way in each tetrahedral–octahedral–tetrahedral unit layer (Guggenheim & Bailey 1975). Figure 2d illustrates another possibility, $C\bar{1}$, compatible with the principle of aluminum avoidance. For $1M$ micas in which Al:Si equals 1:3, the structures represented by Figures 2a, b, c and d can only account for the 'average' or statistical distribution of Al and Si atoms. These space groups cannot be used to illustrate the actual distribution of Al and Si atoms in any one cell volume of a structure.

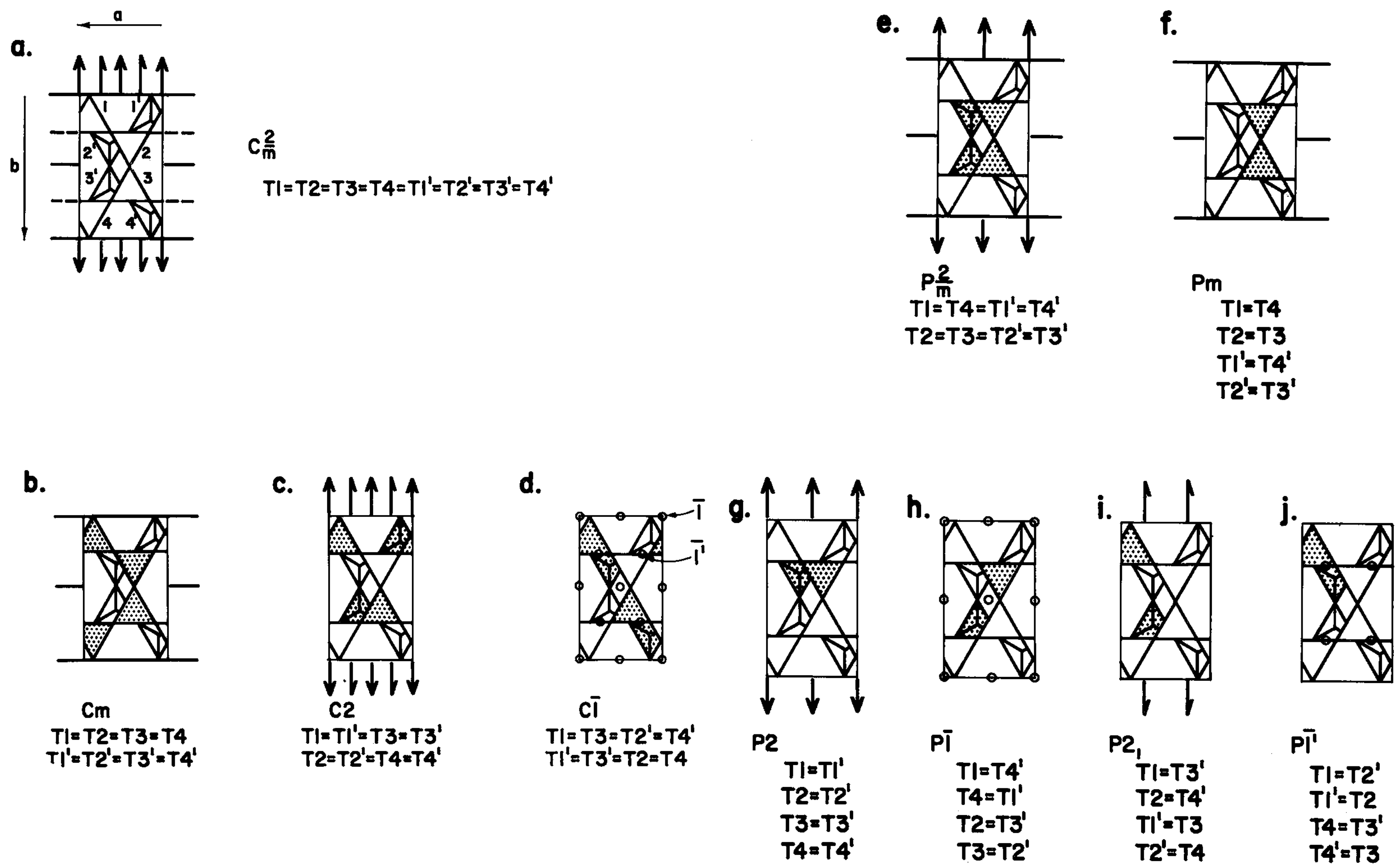

FIG. 2. Projection of the ideal 1*M* mica structure onto the (001) plane. Only the tetrahedral cation sites are shown. The tetrahedra in the upper sheet are numbered 1, 2, 3, 4; the tetrahedra in the lower sheet are numbered 1′, 2′, 3′, 4′. a. The holosymmetric space-group *C*2/*m*. b, c, d. Other *C*-centred structures. e, f, g, h, i, j. Primitive unit-cell structures. Except for *C*2/*m*, in each structure, one set of symmetrically equivalent sites is stippled. For *C*2/*m*, all sites are equivalent.

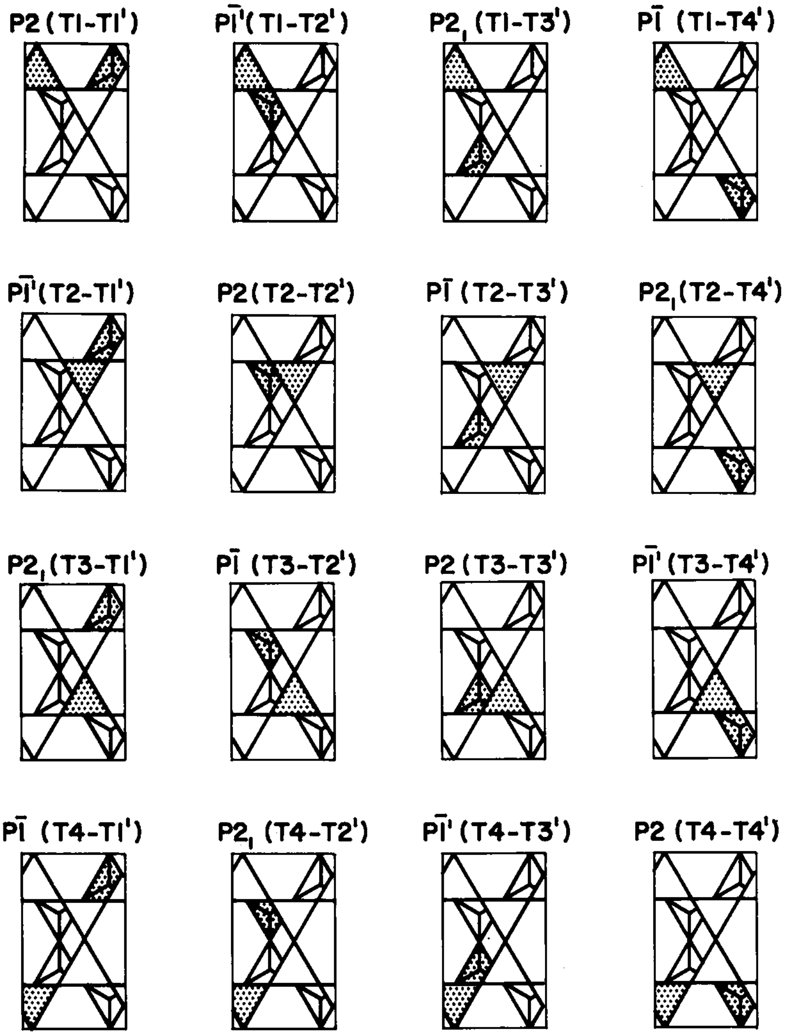

FIG. 3. The complexions of the symmetry types $P2_1$, $P2$, $P\bar{1}$, $P\bar{1}'$. In each case, one set of symmetrically equivalent Al′ sites is stippled.

Within a single unit-cell volume, the distribution of Al and Si atoms must correspond to one of the primitive structures $P2$, $P\bar{1}$, $P2_1$ or $P\bar{1}'$ (Fig. 2g, h, i, j). Note that there are two distinct types of primitive centrosymmetric triclinic Al–Si ordered structures, here designated $P\bar{1}$ and $P\bar{1}'$. The $P2/m$ structure (Fig. 2e), in which there are only two types of sites, $T1 = T1' = T4 = T4'$ and $T2 = T2' = T3 = T3'$, can be discounted for two reasons. Firstly, the multiplicities of the two sites (4 each) are not compatible with an Al:Si ratio of 1:3 in 1M trioctahedral micas. $P2/m$ cannot represent the arrangement of Al and Si atoms in one unit-cell volume in which Al:Si equals 1:3. Secondly, the structure precludes compliance with the aluminum-avoidance principle, except where the space group represents a statistical average of different orientations of some lower-symmetry structure such as $P\bar{1}$, $P2$ or $P\bar{1}'$. The $P2_1/m$, $P2/a$ and $P2_1/a$ structures (not shown in Fig. 2) can be discounted for the same reasons. The unit-cell type Pm (Fig. 2f) is unlikely because if the Al atoms are in any of the four types of sites ($T1 = T4$, $T2 = T3$, $T1' = T4'$ or $T2' = T3'$) the resulting structure of Pm cells alone violates the aluminum-avoidance principle. The Pa structure (not shown in Fig. 2) would also violate the aluminum-avoidance principle. The four remaining unit-cell symmetries, $P2$, $P\bar{1}$, $P2_1$ and $P\bar{1}'$ (Fig. 2g, h, i, j)

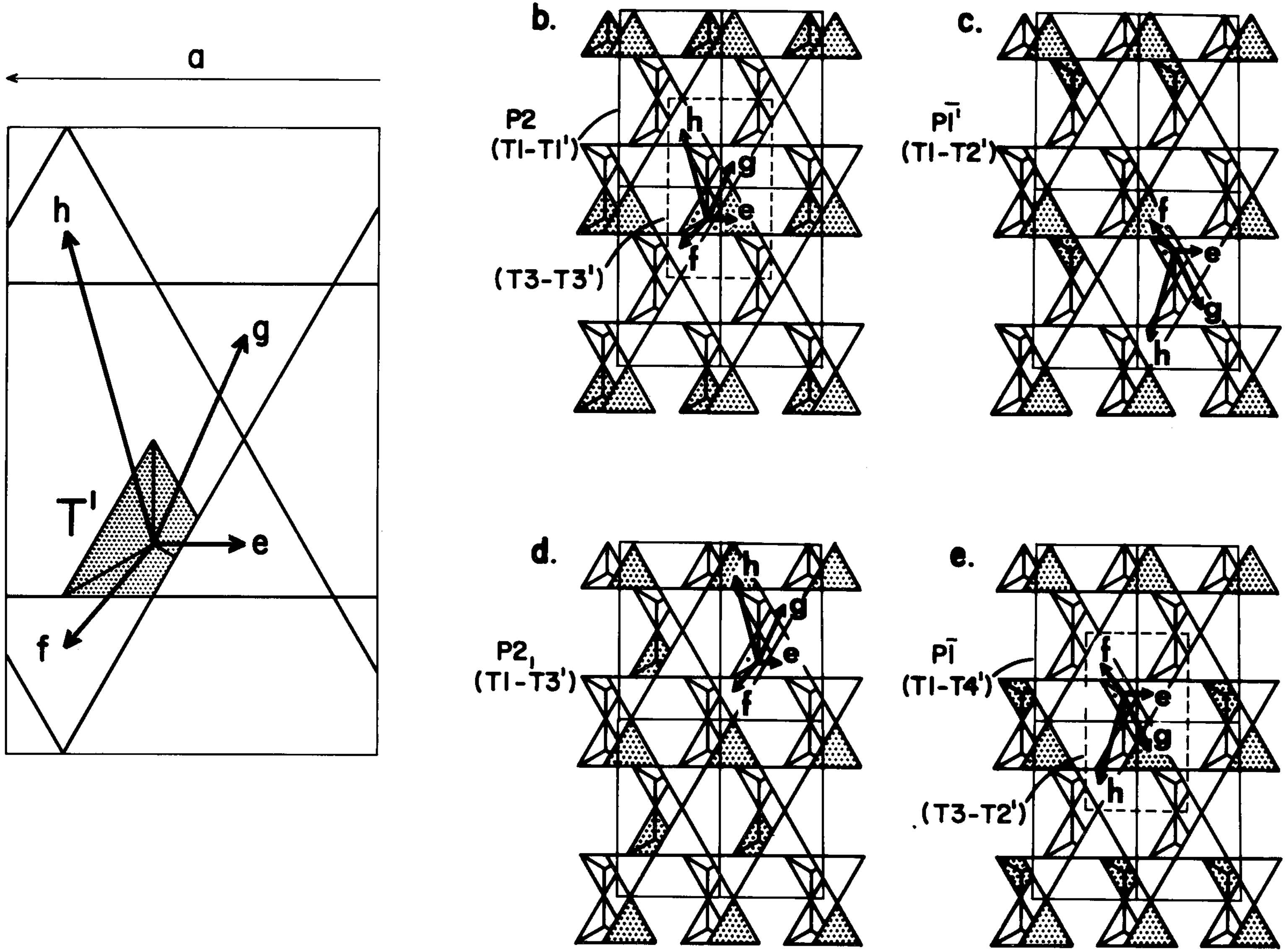

FIG. 4a (left). The four vectors of the type (T–T'), where T' is a tetrahedral site in the lower sheet and T is a tetrahedral site in the upper sheet. Formulae for calculating the (T–T') distances, e, f, g and h are presented in Table 1. b, c, d, e. The ($T = T'$) distances for each of the symmetry types $P2$, $P\bar{1}'$, $P2_1$, and $P\bar{1}$. The stippled tetrahedra are occupied by Al.

are possible, but not necessarily equally likely, as will be demonstrated in the next section.

Figure 3 shows, in matrix form, the four complexions of each unit-cell type $P2$, $P\bar{1}$, $P2_1$ and $P\bar{1}'$. Each complexion of each unit-cell type is designated by the tetrahedral sites occupied by the 2 Al atoms in the unit cell. Hence, $P2$ can be represented by *T1*–*T1*′, *T2*–*T2*′, *T3*–*T3*′, *T4*–*T4*′, the principal diagonal of the matrix. $P\bar{1}$ is represented by *T4*–*T1*′, *T3*–*T2*′, *T2*–*T3*′ or *T1*–*T4*′. $P\bar{1}'$ is represented by *T2*–*T1*′, *T1*–*T2*′, *T4*–*T3*′ or *T3*–*T4*′. And $P2_1$ is represented by *T3*–*T1*′, *T1*–*T3*′, *T4*–*T2*′ or *T2*–*T4*′ Complexions of the same symmetry are related to one another by at least one symmetry element (A_2, *m* or *i*) with or without a translation. For instance, $P\bar{1}$ (*T4*–*T1*′) is related to $P\bar{1}$ (*T1*–*T4*′) by rotation, whereas $P\bar{1}$ (*T1*–*T4*′) is related to $P\bar{1}$ (*T2*–*T3*′) by rotation plus translation (½*a* + ½*b*).

Because all complexions of a given symmetry-type have the same energy, the four complexions of a given symmetry-type are equally likely in an actual structure composed of domains of one symmetry-type. The domains would be related by twinning or antiphase boundaries. If the domains are sufficiently small, the diffraction symmetry may show the average of the four complexions, which is $C2/m$.

THE MOST FAVORABLE SYMMETRY-TYPE

Although all complexions of a symmetry type have the same energy and are, therefore, equally likely, it does not follow that all symmetry types are energetically the same. This should be obvious, if for no other reason than the distances between tetrahedrally co-ordinated aluminum atoms differ from one symmetry type to another.

Other factors considered equal, however small the energy differences, the symmetry types are distinguished on the basis of the distance between an Al atom in one sheet and the nearest Al atom in the other sheet in the same unit-layer. Regardless of the effectiveness of screening by octahedrally co-ordinated cations of the electrostatic interaction between *T* and *T*′ sites, the energy differences between the four symmetry types must be related, at least indirectly, to the relative positions of the Al atoms. According to the principle of aluminum avoidance (Loewenstein 1954) and charge-balance considerations (Güven 1971), the most stable structure maximizes the distances between tetrahedrally co-ordinated Al atoms. Because the *T*–*T*′ interactions are ultimately electrostatic, it may be assumed that the importance of a particular interaction is inversely proportional to the distance between the *T* and *T*′ cations. It is convenient to design an ordering factor, OF, that behaves like an energy function and is minimized for the most favorable (*i.e.*, most stable) Al–Si arrangement. For this reason, the OF is formulated in terms of inverse interatomic distances in the following way for one unit cell having the ideal Al:Si ratio of 1:3.

$$\mathrm{OF} = (\mathrm{Al{-}Al'})^{-1} - \Sigma_{\mathrm{Si}}^{3}\,(\mathrm{Si{-}Al'})^{-1}$$

The $(\mathrm{Al{-}Al'})^{-1}$ term is the inverse of the distance between a reference Al′ in the 'lower' sheet and the closest Al in the 'upper' sheet. Each $(\mathrm{Si{-}Al'})^{-1}$ term is the inverse of the distance between the reference Al′ and one of the three Si atoms in the upper sheet. The formulation behaves like an energy function wherein the unfavorable Al–Al′ interaction has a positive contribution and the favorable Si–Al′ interactions have negative contributions.

TABLE 2. EQUATIONS FOR T-T' AND EVALUATION OF O.F. FOR AN IDEAL 1M MICA

	EXAMPLE MICA	
	a = 5.3 Å, b = $3^{\frac{1}{2}}$ x 5.3 Å, c = 10.15 Å, β = 100°	
T - T'	T - T'	$(T - T')^{-1}$
$f = \sqrt{(0.56\ c\ \sin\beta)^2 + (0.35\ a + 0.56\ c\ \cos\beta)^2 + (b/6)^2}$	5.87 Å	0.170 $Å^{-1}$
$e = \sqrt{(0.56\ c\ \sin\beta)^2 + (0.15\ a - 0.56\ c\ \cos\beta)^2}$	5.88 Å	0.170 $Å^{-1}$
$g = \sqrt{(0.56\ c\ \sin\beta)^2 + (0.15\ a - 0.56\ c\ \cos\beta)^2 + (b/3)^2}$	6.63 Å	0.151 $Å^{-1}$
$h = \sqrt{(0.56\ c\ \sin\beta)^2 + (0.35\ a + 0.56\ c\ \cos\beta)^2 + (b/2)^2}$	7.29 Å	0.137 $Å^{-1}$

$\mathrm{OF} = (\mathrm{Al{-}Al'})^{-1} - \Sigma(\mathrm{Si{-}Al'})^{-1}$

$\mathrm{OF}(P\bar{1}') = f^{-1} - e^{-1} - g^{-1} - h^{-1} = -0.288\ Å^{-1}$

$\mathrm{OF}(P2) = e^{-1} - f^{-1} - g^{-1} - h^{-1} = -0.288\ Å^{-1}$

$\mathrm{OF}(P\bar{1}) = g^{-1} - e^{-1} - f^{-1} - h^{-1} = -0.326\ Å^{-1}$

$\mathrm{OF}(P2_1) = h^{-1} - e^{-1} - f^{-1} - g^{-1} = -0.354\ Å^{-1}$

Figure 4a illustrates the relevant T–T' distances. Table 2 gives the formulae for calculating the different T–T' distances using the atomic co-ordinates for the ideal 1M $C2/m$ mica of Pabst (1955). For some complexions of each symmetry type, it is necessary to select a new set of lattice points, translated by $\frac{1}{2}a + \frac{1}{2}b$, in order that the shortest possible (Al–Al′) distance be within one unit cell and all (T–Al′) distances be of the types shown in Figure 4a and listed in Table 2. Figures 4b and e show complexions of $P2$ and $P\bar{1}$, respectively, for which the lattice must be translated by $\frac{1}{2}a + \frac{1}{2}b$ (dashed unit-cells) for the shortest (Al–Al′) to be within a unit cell. For the purpose of this paper, the values $a = 5.3$ Å, $b = 3^{1/2} \times 5.3$ Å and $d(001) = 10$ Å were used for computing the example values of T–T' and $(T\text{–}T')^{-1}$ in Table 2. Values of OF are also reported for the symmetry types $P2_1$, $P\bar{1}$, $P\bar{1}'$ and $P2$. On the basis of the shortest Al–Al′ interaction alone or the Si–Al′ interactions alone or the OF, the order of the symmetry types is $P2_1$, $P\bar{1}$, $P2 \simeq P\bar{1}'$ in order of decreasing stability.

The OF demonstrates that, whereas there is not an order-of-magnitude difference between any two symmetry types, the differences are significant in comparison with the absolute values of OF. Whereas it is practically obvious by visual inspection of Figure 3 that $P2_1$ is in better agreement with the principle

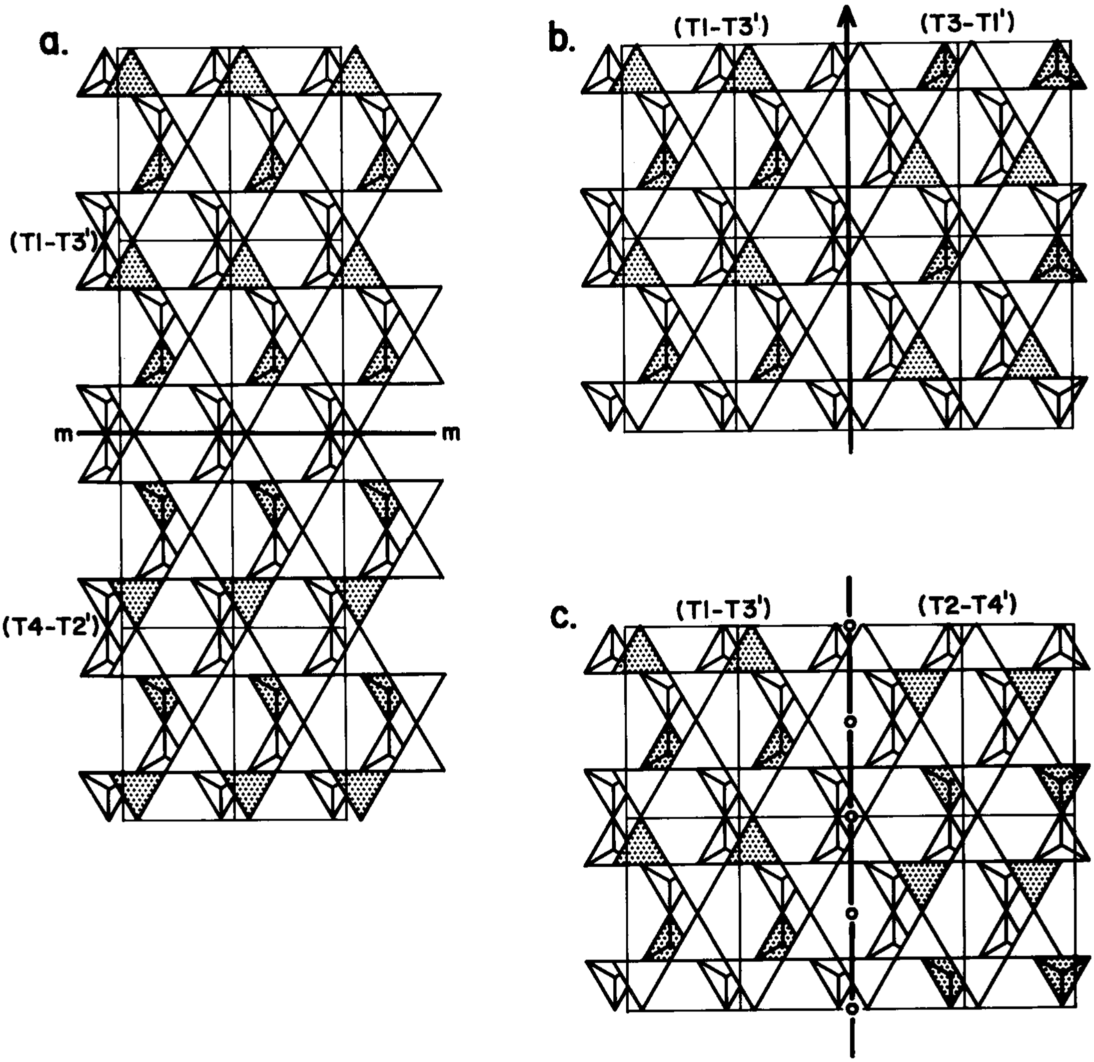

FIG. 5. The different kinds of twinning involving domains of different complexions of $P2_1$. a. The complexions ($T1$–$T3'$) and ($T4$–$T2'$) are related by (010) reflection twinning. b. The complexions ($T1$–$T3'$) and ($T3$–$T1'$) are related by rotational twinning. c. The complexions ($T1$–$T3'$) and ($T2$–$T4'$) are related by inversion twinning.

of aluminum avoidance and Güven's (1971) rule than the other symmetry types, it is not obvious just how much better is the agreement. The OF provides an objective basis for comparing different states of ordering.

The departure of actual structures from Pabst's (1955) ideal $1M$ $C2/m$ mica is small (Radoslovich & Norrish 1962, Hazen & Burnham 1973, McCauley *et al.* 1973, Takeda & Morosin 1975) and is such that the relative position of the tetrahedral sites remains practically ideal. Most of the departure from ideality affects the oxygen atoms in the structure. The equations given in Table 2 for calculating T-T' should apply to any $1M$ mica, ideal or nonideal.

The OF is easily adapted to micas in which Al:Si equals 2:2, such as a hypothetical $1M$ margarite. In the case of $1M$ margarite, there are two space groups compatible with Al–Si ordering, $C2$ and $C\bar{1}$ (Fig. 2c, d). The OF predicts that the $C2$ structure is more stable than $C\bar{1}$. Interestingly, Guggenheim & Bailey (1975) have shown that individual tetrahedral-octahedral–tetrahedral layers in margarite-$2M_1$ are ordered, like in the $C2$ arrangement.

$P2_1$ DOMAINS

Figures 5a, b and c illustrate three kinds of boundaries separating different complexions of the symmetry type $P2_1$. $T1$–$T3'$ and $T4$–$T2'$ domains are related by (010) reflection twinning. $T1$–$T3'$ and $T3$–$T1'$ domains are related by rotation twinning. $T1$–$T3'$ and $T2$–$T4'$ domains are related by inversion twinning. Because the four complexions are energetically identical, all four are likely to occur in natural micas. Hence, the three types of twin boundaries should occur, but may not be equally developed because the twin boundaries are not energetically equal.

In the statistically averaged $1M$ $C2/m$ structures, each unit-cell volume must be ordered according to one of the four symmetry types of Figure 3, most likely as the $P2_1$ symmetry type. The four complexions of $P2_1$ would occur as domains, however small they may be. If sufficiently small, the domain model for $1M$ micas would provide the observed $C2/m$ diffraction-symmetry, which is the combination of the twinning operations and $P2_1$.

CONCLUSIONS

The most stable unit-cell symmetry type for $1M$ micas is $P2_1$. There are four complexions of this symmetry type. The different complexions occur in domains, however small, related by three types of twinning operations.

An ordering factor OF, like the one proposed in this paper, may be useful in predicting the most likely schemes of ordering in other minerals. The OF has the advantage of being purely geometrical, yet it behaves like an energy function, such that the most stable ordered arrangement has the lowest OF. Whereas this approach is not as rigorous as molecular orbital theory, the OF provides adequate results, is simple to calculate and has a sound theoretical basis.

ACKNOWLEDGEMENTS

I thank S.W. Bailey, C.W. Burnham, R.M. Hazen and R.F. Martin for their helpful comments. These individuals are in no way responsible for the shortcomings of the paper, shortcomings which the author acknowledges. W.C. and R. Dewel of the Department of Biology at Appalachian State University provided access to a transmission-electron microscope. I am most grateful to H.Y. McSween, Jr., of the University of Tennessee for performing the electron microprobe analyses. I also thank T. Terranova for drafting the figures and S. Wilson for typing the manuscript. The work was supported by a Kraus-Glass Award from the Mineralogical Society of America.

REFERENCES

DEER, W.A., HOWIE, R.A. & ZUSSMAN, J. (1963): *Rock-Forming Minerals. 3. Sheet Silicates.* John Wiley & Sons, New York.

GATINEAU, P.L. (1964): Structure réelle de la muscovite. Répartition des substitutions isomorphes. *Soc. franç. Minéral. Crist. Bull.* **87**, 321-355.

——— & MÉRING, J. (1966): Relations ordre-désordre dans les substitutions isomorphiques des micas. *Groupe franç. Argiles Bull.* **18**, 67-74.

GUGGENHEIM, S. & BAILEY, S.W. (1975): Refinement of the margarite structure in subgroup symmetry. *Amer. Mineral.* **60**, 1023-1029.

GÜVEN, N. (1971): Structural factors controlling stacking sequences in dioctahedral micas. *Clays Clay Minerals* **19**, 159-165.

HAZEN, R.M. & BURNHAM, C.W. (1973): The crystal structures of one-layer phlogopite and annite. *Amer. Mineral.* **58**, 889-900.

LOEWENSTEIN, W. (1954): The distribution of aluminum in the tetrahedra of silicates and aluminates. *Amer. Mineral.* **39**, 92-96.

MCCAULEY, J.W., NEWNHAM, R.E. & GIBBS, G.V.

(1973): Crystal structure analysis of synthetic fluorophlogopite. *Amer. Mineral.* **58**, 249-254.

PABST, A. (1955): Redescription of the single layer structure of the micas. *Amer. Mineral.* **40**, 967-974.

PAULING, L. (1960): *The Nature of the Chemical Bond* (3rd edition). Cornell University Press, Ithaca, N.Y.

RADOSLOVICH, E.W. & NORRISH, K. (1962): The cell dimensions and symmetry of layer-lattice silicates. I. Some structural considerations. *Amer. Mineral.* **47**, 599-616.

TAKEDA, H. & MOROSIN, B. (1975): Comparison of observed and predicted structural parameters of mica at high temperature. *Acta Cryst.* **B31**, 2444-2452.

______ & ROSS, M. (1975): Mica polytypism: dissimilarities in the crystal structures of coexisting $1M$ and $2M_1$ biotite. *Amer. Mineral.* **60**, 1030-1040.

Received November 4, 1983, revised manuscript accepted February 1, 1984.